The last 59 amino acids of Smoothened cytoplasmic tail directly bind the protein kinase Fused and negatively regulate the Hedgehog pathway.

Sébastien Malpel [1§*], Sandra Claret [1*], Matthieu Sanial [1], Amira Brigui [1], Tristan Piolot [2], Laurent Daviet [3], Séverine Martin-Lannerée [1], Anne Plessis [1**].

[1] « Génétique du Développement et Evolution », Institut Jacques Monod, UMR 7592, CNRS/Universités Paris 6 & 7, 2 Place Jussieu 75251 Paris cedex 05, France

[§] Current address : « Physiologie de l'Insecte : Signalisation et Communication », UMR 1272. INRA/Université Paris VI/INAPG. Centre de Versailles. Route de Saint-Cyr. 78026 VERSAILLES

[2] « Imageries des Processus Dynamiques en Biologie Cellulaire et Biologie du Développement », IFR 117 « Biologie Systémique » - Institut Jacques Monod**,** 2 Place Jussieu 75251 Paris cedex 05, France

[3] Hybrigenics, 3/5 impasse Reille, 75014 Paris, France

* The first two authors equally contributed to this work.

** To whom correspondence should be addressed.

E-mail: plessis@ijm.jussieu.fr

Phone: 33 1 44 27 76 08

Fax: 33 1 44 27 52 68

SUMMARY

The Hedgehog (HH) signalling pathway is crucial for the development of many organisms and its inappropriate activation is involved in numerous cancers. HH signal controls the traffic and activity of the seven-pass transmembrane protein Smoothened (SMO), leading to the transcriptional regulation of HH responsive genes. In *Drosophila*, the intracellular transduction events following SMO activation depend on cytoplasmic multimeric complexes that include the Fused (FU) protein kinase. Here we show that the regulatory domain of FU physically interacts with the 52 last amino-acids of SMO and that the two proteins co-localize *in vivo* within vesicles. The deletion of this region of SMO leads to a constitutive activation of SMO, promoting the ectopic transcription of HH target genes. This activation is partially dependent of FU activity. Thus, we identify a novel link between SMO and the cytoplasmic complex(es) and reveal a negative role of the SMO C-terminal region that interacts with FU. We propose that FU could act as a switch, activator in presence of HH signal or inhibitor in absence of HH.

Key words: Hedgehog, Smoothened, GPCR, Fused, signalling, imaginal disc, Clone 8 cells, *Drosophila* development, two-hybrid, fluorescent imaging.

INTRODUCTION

The Hedgehog signalling proteins act as key morphogens during the development of many organisms as diverse as flies and human (for review see Huangfu and Anderson, 2006; McMahon et al., 2003). In most cases, HH proteins control cell proliferation, differentiation, migration and death in a dose-dependent fashion. In human, disruption of this pathway is associated with congenital abnormalities, and its inappropriate activation plays a central role in the initiation and progression of numerous forms of cancer (for review see Lau et al., 2006; Pasca di Magliano and Hebrok, 2003). HH exerts its influence on cells through a signalling cascade that ultimately regulates the expression of target genes that encode other signalling proteins such as Decapentaplegic (DPP)/TGFβ or Wingless (WG)/WNT, transcription factors such as Engrailed (EN) and the HH receptor Patched (PTC). These transcriptional effects are mediated by zinc finger transcription factors of the GLI family (such as Cubitus interruptus (CI) in fly), which have both repressing and activating functions (Alves et al., 1998; Aza et al., 1997; Motzny and Holmgren, 1995; Nguyen et al., 2005). CI itself is found in at least three forms: a full length form (CI-FL), which is a transcriptional activator, a highly potent and labile activator form (CI-A) and a cleaved form (CI-R), which is a transcriptional repressor. A number of proteins are known to be involved in the control of CI, including the HH receptor PTC (a twelve-pass transmembrane protein) (Nakano et al., 1989) the seven-pass protein Smoothened (SMO) (Alcedo et al., 1996; van den Heuvel and Ingham, 1996) the kinesin-related protein Costal 2 (COS2) (Robbins et al., 1997; Sisson et al., 1997), the F-box/WD protein SLIMB (Jiang and Struhl, 1998), a number of protein kinases (such as Fused (FU) (Preat et al., 1990), the Protein Kinase A (PKA), the Casein Kinase I (CKI) and the Glycogen Synthase Kinase (GSK3) (for review see Price, 2006)) and the pioneer protein Suppressor of Fused (SU(FU)) (Pham et al., 1995).

In the absence of HH signal, the pathway is silenced at multiple levels (for review see Hooper and Scott, 2005; Lum and Beachy, 2004): (i) PTC inhibits SMO, which is endocytosed and undergoes degradation in the lysosome (Denef et al., 2000; Nakano et al., 2004; Zhu et al., 2003); (ii) CI-FL is sequestered in the cytoplasm by both SU(FU) (Methot and Basler, 2000) and microtubule-bound complexes containing FU and COS2 (Stegman et al., 2000; Wang et al., 2000; Wang and Jiang, 2004), leading to its cleavage into CI-R in a proteasome-dependent fashion (Chen et al., 1999). In contrast, in HH receiving cells, HH binding to PTC alleviates its negative effect on SMO, which becomes hyper-phosphorylated and stabilizes at the plasma membrane (Denef et al., 2000). CI is then released from its

cytoplasmic tethering, and its cleavage is inhibited, thus allowing it to transactivate HH target genes. Furthermore, in the cells exposed to the highest levels of HH, both FU and a positive input of COS2 promote formation of the highly potent CI-A form (Alves et al., 1998; Sanchez-Herrero et al., 1996; Wang and Holmgren, 2000).

SMO has several structural and functional characteristics in common with G protein-coupled receptors (GPCR), (Bockaert et al., 2004; Park et al., 2004), such as the ability to interact with β-arrestin (reported in vertebrates only) (Chen et al., 2004) and probably the capacity to dimerize (Hooper, 2003). Nevertheless, SMO displays some atypical features: it does not directly bind any known ligand, and no heterotrimeric G protein has been decisively implicated in the pathway. SMO activity is closely associated with vesicle trafficking, since its targeting to the plasma membrane is sufficient to activate the pathway and endocytosis from the membrane to the lysosome can shut it down (Denef et al., 2000; Nakano et al., 2004; Zhu et al., 2003). Furthermore, SMO reportedly recruits the COS2/CI/FU cytoplasmic complex, probably via a direct interaction with COS2 (Jia et al., 2003; Lum et al., 2003; Ogden et al., 2003; Ruel et al., 2003), suggesting that SMO could directly affect the activity of this complex.

Another positive key member of the HH pathway is the Ser-Thr protein kinase FU. In embryos, FU activity is necessary for the HH-dependent transcription of *wg* during segment polarity establishment (Preat et al., 1990). In wing imaginal discs, it is required along the A/P boundary for the transcription of *en* (Alves et al., 1998; Sanchez-Herrero et al., 1996) and, to a lesser extent, of *ptc* and *dpp* (Glise et al., 2002; Lefers et al., 2001). In all cases, FU antagonizes the negative effects of SU(FU), thus facilitating the entry of CI-FL into the nucleus and allowing its activation in CI-A (Methot and Basler, 2000; Wang et al., 2000). It is composed of two domains: a N-terminal catalytic domain (called FU-KIN) and a C-terminal regulatory domain (called FU-REG) (Figure 1). FU itself is phosphorylated in response to HH stimulation (Therond et al., 1996b) and it can phosphorylate COS2 (Nybakken et al., 2002) and probably SU(FU) (Dussillol-Godar et al., 2006; Ho et al., 2005; Lum et al., 2003), both of them interacting with FU-REG (Monnier et al., 1998; Monnier et al., 2002). FU-REG is required for FU activity, but complex genetic interactions with *su(fu)* and *cos2* indicate that it also participates in the down-regulation of the pathway in the absence of HH signal (Alves et al., 1998; Sanchez-Herrero et al., 1996).

Here, we report that FU can interact directly with SMO in a HH-independent manner *in vivo*. Furthermore, a version of SMO that lacks its FU interaction domain can induce an

ectopic constitutive up-regulation of HH target genes such as *dpp*, *ptc* and also *en* whose expression is characteristic of a high level of HH signalling. Finally, we show that this hyperactivity is independent from the presence of endogenous SMO but partially dependent on the endogenous activity of FU. All together, our data provide evidence of a new link between SMO and the HH-transducing protein complex and reveal a novel level of negative regulation of SMO that is likely mediated by its association with FU.

EXPERIMENTAL PROCEDURES

Plasmids:

pUAST-smo $^{\Delta FU}$ was derived from pUAST-smo (containing a wild-type *smo* cDNA, A.M. Voie and S. M. Cohen) as follows : unmethylated pUAST-smo was digested by XbaI, provoking a deletion from the 2718th nucleotide to the end of the *smo* ORF, instead of which a PCR fragment including nucleotides 2718 to 2951 was cloned. As confirmed by sequencing, the resulting construct corresponds to a deletion from the 977th codon to the end of *smo* ORF.

pAct5C-smo-EGFP, pAct5C-smoΔ^{FU}-EGFP, pAct5C-mRFP-fu, pUAST-m6GFP-fu and pAct5C-mRFP-cos2-expression vectors were constructed by the Gateway recombination method (Invitrogen). The coding sequences (without the termination codon) of *smo*, *fu* and *cos2* cDNAs were amplified by PCR, and cloned in the entry vector pENTR/D-TOPO by directional TOPO Cloning. The resulting plasmids were checked by sequencing. The destination vectors pAWG (pAct5C-GW-EGFP), pARW (pAct5C-mRFP-GW) (where GW is the recombination cassette) were built by T. Murphy and were a gift from him and pUAST-nterm-m6GFP (pUAST-m6GFP-GW) was built and given by A. Brand. All cloning steps were performed according to the manufacturer's instructions. pDAhh was provided by S. Cohen.

Yeast Two-Hybrid Cloning Analysis:

A cDNA fragment encoding the FU regulatory domain (aa 306 to 805) was cloned in the pB27 plasmid (Formstecher et al., 2005), derived from the original pBTM116 (Vojtek and Hollenberg, 1995). A random-primed cDNA library from *Drosophila* embryos (0-24 hours) poly(A$^+$) RNA was constructed into the pP6 plasmid derived from the original pGADGH (Bartel et al., 1993). The library was transformed into the Y187 yeast strain and ten million independent yeast colonies were collected, pooled and stored at –80°C as equivalent aliquot fractions of the same library. The mating protocol has been described elsewhere (Rain et al., 2001). The screen was performed to ensure that a minimum of 50 million interactions were tested. The prey fragments from the positive clones were amplified by PCR and sequenced at their 5' and 3' junctions on a PE3700 Sequencer. The resulting sequences were used to identify the corresponding gene in the GenBank database (NCBI) by a fully automated procedure.

Cell culture and transfection:

Clone-8 (Cl8) cells were cultured as described in van Leeuwen et al. (van Leeuwen et al., 1994). Cells were plated on concanavaline-coated cover glasses during 48h. We then carried out transient transfections using FlyFectin (OZ bioscience). After 24h incubation at 25°C, transfected cells were fixed 30 min with 4% paraformaldehyde.

For RNA interference, double stranded RNA was produced by *in vitro* transcription using T7 polymerase on a PCR product corresponding to residues 2983-3603 of cos2. PCR primers included the T7 promoter: 5' primer: TAATACGACTCACTATAGGGCGAGTGGAAGGAGCGTGTTCTGTCC and 3' primer: TAATACGACTCACTATAGGGCGTTTCGACGACTTGCGTCCTGGATAATTATCTTGT TCTTCTG). RNA interference was performed in S2 cells as described in Worby et al.(Worby et al., 2001) with minor modifications. Transfection of cells (Effectene reagent, Quiagen) with SMO-GFP and RFP-FU fusions was realized after two days and observation two days later.

Fly strains and genetics:

Flies were raised at 25°C. Mutants and transgenic strains are described in the following references: *MS1096* (chr. X, (Capdevila et al., 1994)), *71B* (chr. III, (Brand and Perrimon, 1993)), *da-GAL4* (chr. III (Wodarz et al., 1995)), *hsp-flp ; +/+ ; tub1>CD2>GAL4, UAS-GFP /TM3 (Pignoni and Zipursky, 1997)*, fu^{1}, fu^{RX2} and fu^{M1} (Therond et al., 1996a).

Two *UAS-GFP-smo* strains were used: one (chr. II, used in Figures 2, 3, 4 and 6) was received from J. Jiang (Jia et al., 2003), and the other (chr. III, used in Figures 5 and 3S) was obtained by mobilization of the *UAS-GFP-smo* from a strain donated by A. Zhu (Zhu et al., 2003) and chosen for the stronger expression of the transgene than in the original strain (based on eye color and *in situ* GFP detection).

Transgenic, *UAS-GFP-fu* and *UAS-*$smo^{\Delta FU}$ strains were obtained following the standard P-element-mediated procedure. The *UAS-GFP-fu* construct was validated by rescue of different *fu* mutants (Supplementary Data, Figure 1S). Five *UAS-*$smo^{\Delta FU}$ strains were obtained, and they all induced a higher de-regulation of the pathway than the *UAS-smo* control strains. The same insertion (called T4-5F) was used in all figures.

For clonal over-expression, *hsp-flp ; +/+ ; tub1>CD2>GAL4, UAS-GFP/UAS-smo or pUAS-*$smo^{\Delta FU}$ third instar larvae were heat-shocked for one hour at 37°C. Mosaic analysis with a repressible cell marker (MARCM) (Lee and Luo, 2001) was done in larvae issued from

crosses between UAS-CD8-GFP, *hsp-flp ; tub gal80, FRT40A ; tub GAL4/TM6B* females (a gift from S. Cohen) and FRT *40A smoD16/ CyO ; UAS smo*$^{\Delta FU}$ (T4-5F)/TM6B males.

Imaginal discs immuno-staining:

Imaginal discs from third instar wandering larvae were dissected in PBS; fixed 30 min at room temperature (RT) in 4% paraformaldehyde, washed and permeabilized 3 times for 10 min in PBS + 0.3% Triton (PBST). They were incubated for one hour in PBST + 2% BSA and then overnight at 4°C with the primary antibody, washed 3 times for 10 min with PBST, blocked for 1 hour in PBST+ 2% BSA and incubated for 3 hours at RT with the secondary antibody (in PBST + 2% BSA). Finally, they were rinsed 3 times for 10 min in PBST before being mounted in Cytifluor. GFP was detected in disc merely fixed in parformaldehyde, without any detergent.

Primary antibodies were: anti-PTC, 1/100 (Capdevila and Guerrero, 1994), anti-EN, 1/1000 (4D9, from the Development Studies Hybridoma Bank (DSHB) (Patel et al., 1989)), anti-SMO, 1/1000 (20C6, from DSHB, (Lum et al., 2003), rat anti-CI , 1/5 (2A1, (Motzny and Holmgren, 1995), rabbit polyclonal anti-β-galactosidase, 1/1000 (from ICN/Cappel). The first four antibodies were mouse monoclonal antibodies. Secondary antibodies were from the Jackson Immuno Research Laboratory and were all used at 1/200.

Fluorescence imaging and analysis

All presented images of wing imaginal discs were acquired using a Leica-SP2-AOBS microscope (NA 1,25, objective 40x). Excitation and emission settings were selected as follows: GFP (ex: 488 nm, em: 504-538 nm), Cy3, mRFP (ex: 543 nm, em: 555-620 nm), Cy5 (ex: 633 nm, em: 650-750nm). Images were sampled using a maximum xy pixel size of 100 nm, and z stack were acquired using a 2 µm sampling. Xz view reconstructions were obtained using ImageJ software (Rasband, W.S., ImageJ, U. S. National Institutes of Health, Bethesda, Maryland, USA, http://rsb.info.nih.gov/ij/ 1997-2005).

Cell culture images were acquired with a Yokogawa spinning disk confocal head coupled to a Leica inverted microscope (NA 1,4, objective 100x) (Leica, DMIRB). Excitation was achieved by using an Argon-Kripton RYB 75 mw Laser (Melles Griot). Images were acquired by using a CoolSnap HQ camera (pixel size 6.45 µm) (Princeton Instrument). The whole set up was driven by Metamorph 6.3 (Universal Imaging). The integration and wavelength switch

module was designed by the firm “Errol” and the Institut Jacques Monod imaging facility. Excitation and emission settings were selected as follows: GFP (ex: 488 nm, em: 495-525 nm), mRFP (ex: 568 nm, em : 580, 530).

We processed vesicle segmentation using ImageJ intensity threshold and edge detection functions.

To quantify the vesicular intensity fraction, the integrated intensity of vesicles was determined on each plane and the same procedure was used to determine total cytoplasmic fluorescence. Vesicular intensity fraction was obtained by calculating ratio of these two intensity values.

To determine the proportions of green, red and co-labelled vesicles, we used the ImageJ 3D object Counter plugin (Fabrice Cordelières, Institut Curie, Orsay). We compared the binary images of both channels to estimate the mono- or co-labelled vesicle state of 10 different cells.

The distribution profile of co-labelled vesicles was analyzed by determining the Pearson coefficient on all pixels of these vesicles with the Mandels Coefficient plugin (Tony Collins, Cell Imaging Facility, University Health Network Research). To determine the robustness of the Pearson coefficient results, we did the same analysis after spatial randomization of the red channel using a fay translation method.

RESULTS AND DISCUSSION

SMO C-terminus interacts with FU regulatory domain.

The intracellular C-terminal tail of SMO (SMO-cytotail) has been previously shown to directly associate with COS2 and to co-immunoprecipitate FU, CI and, to a lesser extent, SU(FU) (Jia et al., 2003; Lum et al., 2003; Ogden et al., 2003; Ruel et al., 2003). In a two-hybrid screen using the last 500 amino acids of FU (amino acids (aa) 306 to 805, FU-REG) as a bait, one of the most frequently encountered partners corresponded to the SMO-cytotail. Indeed, we identified 15 independent clones encoding SMO-cytotail (Figure 1). In comparison, 25 independent clones were found to encode COS2 and only 3 SU(FU) (Formstecher et al., 2005; http://pim.hybrigenics.com/pimriderext/droso/index.html). All the SMO-encoding clones overlap and the smallest one defines a minimal region of SMO that is sufficient for its interaction with FU and corresponds to its last 52 amino acids (aa 985 to 1036).

Thus, our data show that the SMO C-terminus can interact directly with FU. This interaction almost certainly occurs independently of COS2 in yeast, since no *cos2* homolog is present in this the genome of *Saccharomyces cerevisiae*.

Apical accumulation of SMO and FU in wing imaginal discs.

HH induces the stabilization of SMO and its relocalization from vesicles to the plasma membrane (Alcedo et al., 2000; Denef et al., 2000; Jia et al., 2003; Nakano et al., 2004; Zhu et al., 2003). In wing imaginal discs, FU was reported to be mostly cytoplasmic (Methot and Basler, 2000). Here, in order to compare the subcellular localizations of SMO and FU, we monitored each protein tagged with Green Fluorescent Protein (GFP) expressed (using *MS1096* driver) in the columnar epithelium of the wing imaginal disc and in the salivary glands (Figure 2). GFP fluorescence was directly observed after fixation of the disc, without treatment by detergents to ensure that any intracellular structures that might be sensitive to these latter were preserved. As expected, GFP-SMO was mostly present in vesicles and at the cell surface (Figure 2B and 2C). Anterior and posterior vesicles may differ in nature since they seem to differ in size, with larger vesicles in the anterior region. Furthermore, comparing different sections throughout the imaginal disc revealed that these vesicles were more abundant in the apical region of the cells. This preferential accumulation of GFP-SMO at the apical region was confirmed by xz view reconstruction (Figure 2D). These results contrast

with the accumulation of SMO at the baso-lateral surface reported by Denef *et al.* (Denef et al., 2000). We checked the orientation of the discs by different methods (see Material and Methods, Figure 2S in Supplementary Data and data not shown), and the same distribution was observed by immunodetection of endogenous SMO. Therefore, the discrepancy between our results and the published data is likely not due to the use of a fusion protein nor to overexpression conditions and is probably due to differences in the experimental conditions, either in the antibody or in the detergent used.

After checking that the *UAS-GFP-fu* construct was indeed able to rescue the effect of *fu* mutants (see Material and Methods and Figure 1S in supplementary data), we also monitored GFP-FU in wing discs. It preferentially accumulated in the anterior compartment (Figures 2E and 3A), as it was reported for endogenous FU (Ruel et al., 2003). At the subcellular level, it was diffusely distributed in the cytoplasm and also accumulated both at the plasma membrane on the apical side and in scattered punctuate structures elsewhere in the cell (see xy sections in Figure 2F and G and xz view reconstruction in Figure 2H). In salivary glands, which are composed of large cells and have the capacity to respond properly to HH signal (Zhu et al., 2003), GFP-FU had a similar distribution (Figure 2I). It was diffuse in the cytoplasm with a greater accumulation at the plasma membrane and in discrete puncta. Moreover, some accumulation was also seen in and around the nucleus, suggesting that FU might play a role in this compartment.

In conclusion, both SMO and FU proteins can be found in punctuate structures. Furthermore, the enrichment of these FU or SMO structures in apical region of the cells likely reflects their polarized traffic towards the apical side where the extra-cellular HH signal is present.

FU and SMO co-localize *in vivo*

To better study SMO/FU co-localization, we pursued our analysis in transfected Cl8 cultured cells, whose size facilitates subcellular observations and which are capable of responding to the HH signal (Chen et al., 1999). We transiently expressed FU tagged with the monomeric Red Fluorescent Protein (mRFP-FU) and SMO tagged with GFP (SMO-GFP), separately (Figure 3D and E) or together (Figure 3G-G"). Confirming the wing disc data, SMO alone accumulated in vesicles, while FU was present both diffusely in the cytoplasm and in small vesicle-like structures. We estimated that about 44% (+/- 13%) of total FU intensity accumulated in these structures (see Table I). We did not determine the nature of the

FU-containing punctuate structures, but they probably correspond to vesicles, since (i) published cell fractionation experiments have demonstrated that FU is indeed partially associated to the vesicular cytoplasmic pool (Ruel et al., 2003, Stegman et al., 2004), (ii) a large number of these structures also contain SMO (see below) which was shown to be vesicular (Nakano et al., 2004) and (iii) their distribution is affected by HH signal (to be published elsewhere).

FU co-expression did not significantly affect the localization of SMO. Conversely, while co-expression of SMO did not significantly change the intensity fraction of FU in vesicular structures (40% +/- 14%, see Table I), the FU-containing structures appeared to be fewer but larger (Figure 3G). According to the labelling profile (Figure 3G"), we estimated (Table I) that 53% of the vesicles were co-labelled with both proteins (SMO+ FU+, yellow arrow), while 25% of vesicles contained only SMO (SMO+ FU-, red arrow) and 22% only FU (SMO- FU+, green arrow). Furthermore, we analyzed the co-localization in SMO+ FU+ vesicles by determining the distribution profile correlation using Pearson Coefficient. We obtained a value of 0.845 ± 0.042 which, compared to the value of - 0.062 ± - 0.028 after randomization, shows a coherent distribution of both proteins and thus demonstrates their co-localization.

Next, we followed both GFP-FU (driven by *MS1096*) and endogenous SMO in the wing imaginal discs (Figure 3 A-C"). The small size of the cells and the use of detergent, which somewhat reduced the detection of punctate FU and SMO (Figure 3B-C"), made subcellular analysis more difficult. Nevertheless, in the posterior compartment (where HH is present), a large number of GFP-FU vesicle structures co-localized with endogenous SMO (Figure 3C-C"). In the anterior compartment where HH is absent, FU was also present in SMO-containing vesicles, but due to a lesser accumulation of SMO, the signal was weaker (Figure 3 B-B").

In conclusion, in both cultured cells and wing imaginal discs, SMO and FU partially co-localize in vesicles. As shown for COS2/SMO association (Ogden et al., 2003), co-localization of SMO/FU is not inhibited by HH (data not shown). The presence of FU in the vesicular structures lacking SMO might occur *via* COS2, since FU has been shown to interact and co-localize with COS2 (Monnier et al., 2002), which can associate with membranes in a SMO-independent manner (Stegman et al., 2004).

SMO controls FU subcellular localisation.

To examine the importance of the SMO/FU interaction *in vivo*, we designed a mutant of SMO ($SMO^{\Delta FU}$) lacking its last 59 residues and thus its region of interaction with FU (see above). In Cl8 cells, $SMO^{\Delta FU}$ tagged with GFP is mostly vesicular (Figure 3F), and its localization was unaffected by FU over-expression, like wild-type SMO. In contrast, $SMO^{\Delta FU}$ over-expression leads to a decrease in the fraction of vesicular FU intensity to 10% (± 7%) of total FU intensity (Table 1 and Figure 3H). This reduction indicates that $SMO^{\Delta FU}$ can affect FU in a dominant negative fashion, probably by impeding its recruitment by endogenous SMO. Such an effect might reflect a dimerization between $SMO^{\Delta FU}$ and the endogenous wild-type SMO proteins, since it was previously suggested that SMO could homodimerize (Hooper, 2003). Alternatively, it might be due to the titration of a third partner that is possibly necessary for vesicular localization of FU. The percentage of vesicles containing $SMO^{\Delta FU}$ alone reached 88%, whereas only 10% of the vesicles contained FU alone and only 2% contained both proteins. Furthermore, as attested by a Pearson correlation coefficient of 0.053 ± - 0.051 (compared with - 0.266 ± - 0.038 after randomization), no co-localization was seen within the few co-labelled $SMO^{\Delta FU}$+ FU+ vesicles.

In summary, the last 59 residues of SMO not only directly bind FU but are also necessary *in vivo* to recruit FU to vesicles. This suggests that the co-localization observed between SMO and FU is likely due to their interaction *in vivo.* The co-localization of SMO/FU might, however, be mediated by their respective interactions with COS2. The FU-binding region of SMO (aa 985-1036) is distinct from its COS2-binding region (aa 557-686) previously defined by two-hybrid assays (Lum et al., 2003), but it is included within a region of SMO (aa 818-1035, $SMO^{818\text{-}1035}$) that is sufficient to allow co-immunoprecipitation of COS2 (Jia et al., 2003), although this latter interaction was not shown to be direct. We expressed mRFP-COS2 alone or with either SMO-GFP or $SMO^{\Delta FU}$-GFP in Cl8 cells (see Supplementary data, Figure 3S). In all cases, mRFP-COS2 was present in punctate structures, but did not co-localize with SMO (or with $SMO^{\Delta FU}$). However, in the presence of HH. mRFP-COS co-localized at the plasma membrane with either SMO or $SMO^{\Delta FU}$, indicating that the last 59 amino-acids of SMO are not required for SMO/COS2 co-localization. Last, we showed that SMO/FU co-localization was not affected when the accumulation of COS2 was strongly reduced by RNA interference (Figure 4). For all these reasons, we conclude that it is very unlikely that endogenous COS2 bridges SMO and FU and that the co-localization of SMO/FU reflects their interaction in Cl8 cells.

Thus, FU has the ability to directly bind both COS2 and SMO. Moreover, the co-expression of FU with SMO and COS leads to the localization of COS2 in SMO-containing vesicles (unpublished data). It is therefore likely that the reported co-immunoprecipitation between COS2 and $SMO^{818-1035}$ occurs indirectly *via* their respective associations with FU (Jia et al., 2003). This interpretation is further supported by the fact that the amount of COS2 co-immunoprecipated with SMO was reported to be strongly increased by the co-expression of FU

Loss of the FU-interacting domain turns SMO into a potent constitutive activator.

It is clear that multiple interactions can take place between the SMO, FU and COS2 proteins (Jia et al., 2003; Lum et al., 2003 ; Monnier et al., 1998; Monnier et al., 2002; Ogden et al., 2003; Sisson et al., 1997). Although such multiple associations might simply play an architectural role in reinforcing the stability of the complex, it is also possible that each interaction plays a specific role. We assessed the functional relevance of SMO/FU interaction *in vivo* by comparing the effects of SMO and $SMO^{\Delta FU}$ over-expression on wing development. We used two drivers *MS1096* and *71B,* the latter also being broadly expressed, albeit at a lower level, throughout the wing pouch. As expected, GFP-SMO over-expression has a relatively mild effect, consistent with a low level of activation of the HH pathway in the anterior compartment of the disc: all the wings display extra cross-veins between the longitudinal veins (LV) LV2 and LV3, an enlargement of LV3-LV4 spacing and a thickening of vein LV3 (Figure 5B-C). Similar effects were previously reported with various *UAS-smo* and *UAS-GFP-smo* transgenes (Hooper, 2003; Nakano et al., 2004; Zhu et al., 2003). In contrast, over-expression of $SMO^{\Delta FU}$ induces strong wing defects (Figure 5D, E) characterized by numerous extra cross-veins and ectopic LV3 vein tissue with extra campaniform sensillae (data not shown) in the anterior compartment. Moreover, when the wing patterning was not too severely disturbed, an enlargement of LV3-LV4 intervein could also be observed (see Figure 6B). The more severely affected flies could not emerge and the wings of the dissected imago were almost circular with the anterior region invaded by vein tissue (Figure 5E). Such phenotypes are indicative of a high level of ectopic activation of the HH pathway and are similar to those reported for the over-expression of some gain of function *smo* mutants (Zhang et al., 2004). Multiple independent *UAS-smo* transgenes (wild-type and tagged versions) were tested in different laboratories and their expression led to low levels of HH pathway activation (independently from the presence or absence of the GFP

moety) (Hooper, 2003; Nakano et al., 2004; Zhu et al., 2003, Zhang et al., 2004, Apionishev et al., 2004). One report indicates that, at most, one in six lines has an unusually high effect, due to a higher level of expression (Hooper, 2003). Here, for all $SMO^{\Delta FU}$strains tested the effect was medium to high. We compared several independent $smo^{\Delta FU}$ and *smo* insertions (including a novel insertion which we selected for high expression). $smo^{\Delta FU}$ over-expression always induced a much stronger defect than wild type *smo* over-expression (data not shown). Thus, the difference between SMO and $SMO^{\Delta FU}$ induced phenotypes is probably not due to differences in the levels of transcription of the transgenes. Immunodetection of SMO and $SMO^{\Delta FU}$, revealed however, a difference in the levels of accumulation of the two types of proteins (data not shown). Indeed, as reported for other constitutively active forms of SMO, such as oncogenic SMO variants (Nakano et al., 2004; Zhu et al., 2003), for mutants of SMO that mimic constitutively phosphorylated SMO (Apionishev et al., 2005; Jia et al., 2004; Zhang et al., 2004), or a form of SMO stabilized at the membrane by fusion with a GAP anchor (Zhu et al., 2003), $SMO^{\Delta FU}$ protein accumulated at a higher level than the wild type form of SMO.

Normally, in HH-receiving cells at the A/P boundary, CI-FL accumulates and induces expression of *dpp*, *ptc* and *en*, whereas in the anterior part of the wing pouch, CI-R represses *dpp* and *hh* (Methot and Basler, 1999). Here, in response to over-expression of $SMO^{\Delta FU}$ (driven by *MS1096*), high levels of ectopic expression of *dpp* as well as *ptc* were seen in most of the anterior part of the wing pouch, which is itself greatly enlarged (Figure 6B to B''). In contrast, as previously reported (Hooper, 2003; Jia et al., 2004; Nakano et al., 1989), over-expression of wild type SMO led to only low levels of ectopic expression of *dpp* in the most anterior region of the wing pouch, and had little effect on the expression of *ptc* (Figure 6A to A'', and data not shown). Furthermore, consistent with its action on HH targets, $SMO^{\Delta FU}$ expression leads to a uniform level of CI-FL throughout the anterior compartment (compare Figure 6E and F). We also expressed $SMO^{\Delta FU}$ in clones: transcription of *ptc* and *en* is activated in all clones located in the anterior compartment (even far from the posterior HH source) (Figure 6C-C", D-D"), indicating that a high level of activation can be reached away from the boundary. The effect of $smo^{\Delta FU}$ overexpression on anterior *en* expression contrasts with the failure of even the strongest *smo* transgenes to do so (Hooper, 2003) and provides further evidence of a difference in the activities of the SMO and $SMO^{\Delta FU}$ proteins.

It could have been possible that this up-regulation of HH targets induced by $SMO^{\Delta FU}$ was a secondary effect of an ectopic *hh* expression resulting from a decrease in CI-R, but this was

ruled out by the analysis of SMO$^{\Delta FU}$ over-expression in clones of cells which revealed that the high *ptc* and *en* expression of these clones is cell-autonomous (Figure 6C-C", D-D).

Thus, the 59 amino acid long C-terminal truncation of the SMO cytotail seems to gives rise to an activated, constitutive form of SMO. Another possibility is that SMO$^{\Delta FU}$ activating effects might simply rely on the sequestration or mislocation of antagonists of the pathway, thus allowing the activation of endogenous SMO. Therefore, we tested whether the effects of SMO$^{\Delta FU}$ depended on wild-type endogenous SMO by monitoring the effects of *smo*$^{\Delta FU}$ expression in clones of cells mutant for *smo*. As shown in Figure 6G-G'', SMO$^{\Delta FU}$ was still able to induce the expression of *ptc* and the accumulation of full length CI in the absence of endogenous SMO protein. This indicated that the loss of the last 59 residues leads to the constitutive activation of SMO. Interestingly, a SMO variant whose last 96 amino acids had been deleted (SMO$^{\Delta 939\text{-}1036}$) was shown to have an activity comparable to that of wild type SMO (Nakano et al., 2004). Two regions of the SMO cytotail are thus defined: (i) a region that covers the last 59 amino acids which interacts with FU and inhibits SMO activity in the absence of HH, and (ii) a region that includes amino acids 939 to 977 which is necessary for SMO$^{\Delta FU}$ hyperactivity. None of these regions are required for the activity of full length SMO in response to HH.

In summary, our data show that the last 59 amino acids of SMO can inhibit its activity in the absence of HH signal. Since SMO$^{\Delta FU}$ has lost its capacity to interact directly with FU. We propose that this negative regulation of SMO might occur via its association with FU-REG. In this context, the weakness of wild type SMO over-expression effects can be attributed to its negative control by endogenous FU. Note that such an effect might also partially account for previous genetic data showing that FU-REG can negatively regulate the HH pathway (Sanchez-Herrero et al., 1996, Alves et al., 1998, Lefers et al., 2001, Ascano et al., 2002) .We cannot exclude, however, that the loss of the last 59 amino acids of SMO could lead to SMO hyperactivity independently from the loss of FU binding..

Partial requirement of FU for SMO$^{\Delta FU}$ -induced activation of the HH pathway.

FU thus seems to be a negative regulator of SMO in the absence of HH signal, but extensive genetic and molecular analysis has established a clear positive regulatory role for FU as well (Alves et al., 1998; Preat et al., 1990; Preat et al., 1993). We assessed the participation of FU in the activating effects of SMO$^{\Delta FU}$ and SMO, by over-expressing these

latter in a *fu* mutant background. *fu* wings display a longitudinal fusion of the LV3 and LV4 associated with a posterior expansion of the double row of marginal bristles (Therond et al., 1996b) (Figure 7A). We first tested the effects of fu^{RX2}, a *fu* allele lacking the last 57 codons of the *fu* coding sequence (Robbins et al., 1997). Strikingly, the phenotype induced by either SMO$^{\Delta FU}$ or SMO over-expression are suppressed in fu^{RX2} flies (Figure 7, compare C with B and F with E). This effect is dosage dependent since the loss of one dose of *fu* is sufficient to reduce the SMO$^{\Delta FU}$- or SMO-induced phenotype (Figure 7D). At the A/P boundary, however, the LV3-4 spacing is normal, indicating that, in this region, expression of SMO$^{\Delta FU}$ and SMO can still activate the pathway at a level sufficient to compensate for the effects of the *fu* mutation (Figure 6, compare C and F with A). All these reciprocal suppressive effects are not specific to the *fu* allele: similar results (See Supplementary data, Figure 5S and data not shown) were seen both with fu^{M1},which encodes only the first 80 amino acids of FU and is therefore unlikely to have a residual kinase activity, and with fu^{1}, which has a missense mutation in the kinase domain of FU (Alves et al., 1998; Robbins et al., 1997).

The suppression of the SMO or SMO$^{\Delta FU}$ -induced phenotypes in the *fu* mutants argues that FU is required for SMO or SMO$^{\Delta FU}$ effects on the HH pathway away from the A/P border, while the reciprocal suppression of the *fu* phenotype at the A/P boundary by over-expression of SMO or SMO$^{\Delta FU}$ argues that , when high levels of HH are present, a high level of activation can occur without FU. Thus, SMO$^{\Delta FU}$ and to a lesser extent, SMO, activate the HH pathway in both a FU-dependent and a FU-independent manner. Although, the requirement for FU seems normally restricted to the AP border (where HH levels are highest) for the expression of genes such as *en*, the present data indicate that FU can also be necessary for ectopic activation of the pathway away from the AP border. We propose that FU's normal role is to enhance the level of activation of the pathway in response to HH and that it also does so in presence of high levels of SMO or SMO$^{\Delta FU}$. The loss of FU activity combined with the activating effects of SMO or SMO$^{\Delta FU}$ over-expression result a wild type phenotype.

Lastly, our data also show that, in the absence of FU, SMO can be as potent an activator as SMO$^{\Delta FU}$. Indeed, SMO seems to suppress the effects of *fu* mutations with a similar efficiency to SMO$^{\Delta FU}$. This could reflect the incapacity of FU mutant proteins to bind and/or inhibit SMO. Since this is observed with different *fu* alleles which are all directly (fu^{1}) or indirectly (fu^{RX2}, fu^{M1}) impaired in their catalytic activity, we propose that the negative action of FU on SMO is likely mediated by its kinase activity. FU may, for example, phosphorylate SMO. Such an effect could prevent SMO activation by impeding its activating

hyperphosphorylation by the PKA and the CKI (Apionishev et al., 2005; Jia et al., 2004; Zhang et al., 2004).

CONCLUSION

HH signal appears to act mainly by alleviating or bypassing multiple inhibiting processes that stringently shut down the pathway in the absence of an adequate signal. This occurs through the tight control of the subcellular localization, composition and stability of protein complexes that link the transmembrane protein SMO to the regulators of the transcription factor CI. Here we report that SMO and FU can physically interact, leading to the direct recruitment of FU in SMO-containing vesicles in the absence of HH signal. The deletion of the region of the SMO cytotail required for its interaction with FU leads to a constitutive activation of the pathway. Thus, our data suggest that FU, in addition to its known activator function, can also act as a negative regulator of SMO activity in the absence of HH signal (see the model in Figure 8). Given that SMO activation by HH is known to involve both its hyperphosphorylation by PKA and CKI and changes in its traffic that lead to its stabilization, FU might inhibit SMO activation by acting on either of these stages. Via its dual role, FU may thus not only increase the robustness of the pathway, dampening any noise that might occur in the absence of any signal, but also reinforce the bistable switch properties of the pathway (Lai et al., 2004).

ACKNOWLEDGMENTS

We thank S. Cohen, I. Guerrero, J. Jiang, L. Ruel, F. Schweisguth, P. Thérond, C. Tong, M. van den Heuvel, A.-M. Voie and A. Zhu for providing plasmids, antibodies, fly strains, cell lines and technical advice, and A. Brand and T. Murphy for sharing unpublished material. The monoclonal antibodies obtained from the Developmental Studies Hybridoma bank were developed under the auspices of the NICHD and maintained by the University of Iowa. We are grateful to J. E. Formstecher, A. Zhu and many members of the IJM for advice and stimulating discussions. We also thank C. Leyssales and S. Voegeling for their help in some experiments and all the staff of Hybrigenics for their contribution. We are greatly indebted to C. Lamour-Isnard for her constant support and to M. Coppey, C. Durieux, M. Tramier and C. Chamot for sharing their expertise in fluorescent imaging, to R. Karess, H. Tricoire, and R. Veitia for critical reading of the manuscript. We would like to express our gratitude to R. Karess and A. Kropfinger for linguistic help with the manuscript. This work was supported by the ARC (N°4797), by an ACI “Biologie du development et physiologie integrative” (N°525044) and by a GenHomme Network Grant (02490-6088) (to Hybrigenics and the Institut Curie). The imaging facilities were partially funded by the ARC, the region Ile de France (SESAME) and the University Paris VII. S. M-L and A. B. were the recipients of

MNRT fellowships. S. C. was ATER at the University Paris 7, and was also supported by "Fondation des Treilles".

REFERENCES

Alcedo, J., Ayzenzon, M., Von Ohlen, T., Noll, M., and Hooper, J. E. (1996). The Drosophila smoothened gene encodes a seven-pass membrane protein, a putative receptor for the Hedgehog signal. *Cell* 86, 221-232.

Alcedo, J., Zou, Y., and Noll, M. (2000). Posttranscriptional regulation of smoothened is part of a self-correcting mechanism in the Hedgehog signaling system. *Mol Cell* 6, 457-65.

Alves, G., Limbourg, B. B., Tricoire, H., Brissard, Z. J., Lamour, I. C., and Busson, D. (1998). Modulation of Hedgehog target gene expression by the Fused serine-threonine kinase in wing imaginal discs. *Mech Dev* 78, 17-31.

Apionishev, S., Katanayeva, N. M., Marks, S. A., Kalderon, D., and Tomlinson, A. (2005). Drosophila Smoothened phosphorylation sites essential for Hedgehog signal transduction. *Nat Cell Biol* 7, 86-92.

Ascano, M., Jr., Nybakken, K. E., Sosinski, J., Stegman, M. A., and Robbins, D. J. (2002). The carboxyl-terminal domain of the protein kinase fused can function as a dominant inhibitor of hedgehog signaling. *Mol Cell Biol* 22, 1555-66.

Aza, B. P., Ramirez, W. F., Laget, M. P., Schwartz, C., and Kornberg, T. B. (1997). Proteolysis that is inhibited by hedgehog targets Cubitus interruptus protein to the nucleus and converts it to a repressor. *Cell* 89, 1043-53.

Bartel, P., Chien, C. T., Sternglanz, R., and Fields, S. (1993). Elimination of false positives that arise in using the two-hybrid system. *Biotechniques* 14, 920-4.

Bockaert, J., Roussignol, G., Becamel, C., Gavarini, S., Joubert, L., Dumuis, A., Fagni, L., and Marin, P. (2004). GPCR-interacting proteins (GIPs): nature and functions. *Biochem Soc Trans* 32, 851-5.

Brand, A. H., and Perrimon, N. (1993). Targeted gene expression as a means of altering cell fates and generating dominant phenotypes. *Development* 118, 401-15.

Capdevila, J., and Guerrero, I. (1994). Targeted expression of the signaling molecule decapentaplegic induces pattern duplications and growth alterations in Drosophila wings. *Embo J* 13, 4459-68.

Capdevila, J., Pariente, F., Sampedro, J., Alonso, J. L., and Guerrero, I. (1994). Subcellular localization of the segment polarity protein patched suggests an interaction with the wingless reception complex in Drosophila embryos. *Development* 120, 987-98.

Chen, C. H., von Kessler, D., Park, W., Wang, B., Ma, Y., and Beachy, P. A. (1999). Nuclear trafficking of Cubitus interruptus in the transcriptional regulation of Hedgehog target gene expression. *Cell* 98, 305-16.

Chen, W., Ren, X. R., Nelson, C. D., Barak, L. S., Chen, J. K., Beachy, P. A., de Sauvage, F., and Lefkowitz, R. J. (2004). Activity-dependent internalization of smoothened mediated by beta-arrestin 2 and GRK2. *Science* 306, 2257-60.

Denef, N., Neubuser, D., Perez, L., and Cohen, S. M. (2000). Hedgehog induces opposite changes in turnover and subcellular localization of patched and smoothened. *Cell* 102, 521-31.

Dussillol-Godar, F., Brissard-Zahraoui, J., Limbourg-Bouchon, B., Boucher, D., Fouix, S., Lamour-Isnard, C., Plessis, A., and Busson, D. (2006). Modulation of the

Suppressor of fused protein regulates the Hedgehog signaling pathway in Drosophila embryo and imaginal discs. *Dev Biol*. 291,53-66

Formstecher, E., Aresta, S., Collura, V., Hamburger, A., Meil, A., Trehin, A., Reverdy, C., Betin, V., Maire, S., Brun, C., Jacq, B., Arpin, M., Bellaiche, Y., Bellusci, S., Benaroch, P., Bornens, M., Chanet, R., Chavrier, P., Delattre, O., Doye, V., Fehon, R., Faye, G., Galli, T., Girault, J. A., Goud, B., de Gunzburg, J., Johannes, L., Junier, M. P., Mirouse, V., Mukherjee, A., Papadopoulo, D., Perez, F., Plessis, A., Rosse, C., Saule, S., Stoppa-Lyonnet, D., Vincent, A., White, M., Legrain, P., Wojcik, J., Camonis, J., and Daviet, L. (2005). Protein interaction mapping: a Drosophila case study. *Genome Res* 15, 376-84.

Glise, B., Jones, D. L., and Ingham, P. W. (2002). Notch and Wingless modulate the response of cells to Hedgehog signalling in the Drosophila wing. *Dev Biol* 248, 93-106.

Ho, K. S., Suyama, K., Fish, M., and Scott, M. P. (2005). Differential regulation of Hedgehog target gene transcription by Costal2 and Suppressor of Fused. *Development* 132, 1401-12.

Hooper, J. E. (2003). Smoothened translates Hedgehog levels into distinct responses. *Development* 130, 3951-63.

Hooper, J. E., and Scott, M. P. (2005). Communicating with Hedgehogs. *Nat Rev Mol Cell Biol* 6, 306-17.

Huangfu, D., and Anderson, K. V. (2006). Signaling from Smo to Ci/Gli: conservation and divergence of Hedgehog pathways from Drosophila to vertebrates. *Development* 133, 3-14.

Jia, J., Tong, C., and Jiang, J. (2003). Smoothened transduces Hedgehog signal by physically interacting with Costal2/Fused complex through its C-terminal tail. *Genes Dev* 17, 2709-20.

Jia, J., Tong, C., Wang, B., Luo, L., and Jiang, J. (2004). Hedgehog signalling activity of Smoothened requires phosphorylation by protein kinase A and casein kinase I. *Nature* 432, 1045-50.

Jiang, J., and Struhl, G. (1998). Regulation of the Hedgehog and Wingless signalling pathways by the F-box/WD40-repeat protein Slimb. *Nature* 391, 493-6.

Lai, K., Robertson, M. J., and Schaffer, D. V. (2004). The sonic hedgehog signaling system as a bistable genetic switch. *Biophys J* 86, 2748-57.

Lau, J., Kawahira, H., and Hebrok, M. (2006). Hedgehog signaling in pancreas development and disease. *Cell Mol Life Sci* 63, 642-52.

Lee, T., and Luo, L. (2001). Mosaic analysis with a repressible cell marker (MARCM) for Drosophila neural development. *Trends Neurosci* 24, 251-4.

Lefers, M. A., Wang, Q. T., and Holmgren, R. A. (2001). Genetic dissection of the Drosophila Cubitus interruptus signaling complex. *Dev Biol* 236, 411-20.

Lum, L., and Beachy, P. A. (2004). The Hedgehog response network: sensors, switches, and routers. *Science* 304, 1755-9.

Lum, L., Zhang, C., Oh, S., Mann, R. K., von Kessler, D. P., Taipale, J., Weis-Garcia, F., Gong, R., Wang, B., and Beachy, P. A. (2003). Hedgehog signal transduction via Smoothened association with a cytoplasmic complex scaffolded by the atypical kinesin, Costal-2. *Mol Cell* 12, 1261-74.

McMahon, A. P., Ingham, P. W., and Tabin, C. J. (2003). Developmental roles and clinical significance of hedgehog signaling. *Curr Top Dev Biol* 53, 1-114.

Methot, N., and Basler, K. (1999). Hedgehog controls limb development by regulating the activities of distinct transcriptional activator and repressor forms of Cubitus interruptus. *Cell* 96, 819-31.

Methot, N., and Basler, K. (2000). Suppressor of fused opposes hedgehog signal transduction by impeding nuclear accumulation of the activator form of Cubitus interruptus. *Development* 127, 4001-10.

Monnier, V., Dussillol, F., Alves, G., Lamour, I. C., and Plessis, A. (1998). Suppressor of fused links fused and Cubitus interruptus on the hedgehog signalling pathway. *Curr Biol* 8, 583-6.

Monnier, V., Ho, K. S., Sanial, M., Scott, M. P., and Plessis, A. (2002). Hedgehog signal transduction proteins: contacts of the Fused kinase and Ci transcription factor with the kinesin-related protein Costal2. *BMC Dev Biol* 2, 4.

Motzny, C. K., and Holmgren, R. (1995). The Drosophila cubitus interruptus protein and its role in the wingless and hedgehog signal transduction pathways. *Mech. Dev.* 52, 137-150.

Nakano, Y., Guerrero, I., Hidalgo, A., Taylor, A., Whittle, J. R. S., and Ingham, P. W. (1989). A protein with several possible membrane-spanning domains encoded by the *Drosophila* segment polarity gene *patched*. *Nature* 341, 508-513.

Nakano, Y., Nystedt, S., Shivdasani, A. A., Strutt, H., Thomas, C., and Ingham, P. W. (2004). Functional domains and sub-cellular distribution of the Hedgehog transducing protein Smoothened in Drosophila. *Mech Dev* 121, 507-18.

Nguyen, V., Chokas, A. L., Stecca, B., and Altaba, A. R. (2005). Cooperative requirement of the Gli proteins in neurogenesis. *Development* 132, 3267-79.

Nybakken, K. E., Turck, C. W., Robbins, D. J., and Bishop, J. M. (2002). Hedgehog-stimulated phosphorylation of the kinesin-related protein Costal2 is mediated by the serine/threonine kinase fused. *J Biol Chem* 277, 24638-47.

Ogden, S. K., Ascano, M., Jr., Stegman, M. A., Suber, L. M., Hooper, J. E., and Robbins, D. J. (2003). Identification of a functional interaction between the transmembrane protein Smoothened and the kinesin-related protein Costal2. *Curr Biol* 13, 1998-2003.

Park, P. S., Filipek, S., Wells, J. W., and Palczewski, K. (2004). Oligomerization of G protein-coupled receptors: past, present, and future. *Biochemistry* 43, 15643-56.

Pasca di Magliano, M., and Hebrok, M. (2003). Hedgehog signalling in cancer formation and maintenance. *Nat Rev Cancer* 3, 903-11.

Patel, N. H., Martin-Blanco, E., Coleman, K. G., Poole, S. J., Ellis, M. C., Kornberg, T. B., and Goodman, C. S. (1989). Expression of engrailed proteins in arthropods, annelids, and chordates. *Cell* 58, 955-68.

Pham, A., Therond, P., Alves, G., Tournier, F. B., Busson, D., Lamour Isnard, C., Bouchon, B. L., Préat, T., and Tricoire, H. (1995). The Suppressor of fused gene encodes a novel PEST protein involved in Drosophila segment polarity establishment. *Genetics* 140, 587-598.

Pignoni, F., and Zipursky, S. L. (1997). Induction of Drosophila eye development by decapentaplegic. *Development* 124, 271-8.

Preat, T., Therond, P., Lamour, I. C., Limbourg, B. B., Tricoire, H., Erk, I., Mariol, M. C., and Busson, D. (1990). A putative serine/threonine protein kinase encoded by the segment- polarity fused gene of Drosophila. *Nature* 347, 87-9.

Preat, T., Therond, P., Limbourg, B. B., Pham, A., Tricoire, H., Busson, D., and Lamour, I. C. (1993). Segmental polarity in Drosophila melanogaster: genetic dissection of fused in a Suppressor of fused background reveals interaction with costal-2. *Genetics* 135, 1047-62.

Price, M. A. (2006). CKI, there's more than one: casein kinase I family members in Wnt and Hedgehog signaling. *Genes Dev* 20, 399-410.

Rain, J. C., Selig, L., De Reuse, H., Battaglia, V., Reverdy, C., Simon, S., Lenzen, G., Petel, F., Wojcik, J., Schachter, V., Chemama, Y., Labigne, A., and Legrain, P. (2001). The protein-protein interaction map of Helicobacter pylori. *Nature* 409, 211-5.

Robbins, D. J., Nybakken, K. E., Kobayashi, R., Sisson, J. C., Bishop, J. M., and Therond, P. P. (1997). Hedgehog elicits signal transduction by means of a large complex containing the kinesin-related protein costal2. *Cell* 90, 225-34.

Ruel, L., Rodriguez, R., Gallet, A., Lavenant-Staccini, L., and Therond, P. P. (2003). Stability and association of Smoothened, Costal2 and Fused with Cubitus interruptus are regulated by Hedgehog. *Nat Cell Biol* 5, 907-13.

Sanchez-Herrero, E., Couso, J. P., Capdevila, J., and Guerrero, I. (1996). The fu gene discriminates between pathways to control dpp expression in Drosophila imaginal discs. *Mech Dev* 55, 159-70.

Sisson, J. C., Ho, K. S., Suyama, K., and Scott, M. P. (1997). Costal2, a novel kinesin-related protein in the Hedgehog signaling pathway. *Cell* 90, 235-45.

Stegman, M., Vallance, J., Elangovan, G., Sosinski, J., Cheng, Y., and Robbins, D. (2000). Identification of a tetrameric hedgehog signaling complex. *J Biol Chem* 275, 21809-12.

Stegman, M. A., Goetz, J. A., Ascano, M., Jr., Ogden, S. K., Nybakken, K. E., and Robbins, D. J. (2004). The Kinesin-related protein Costal2 associates with membranes in a Hedgehog-sensitive, Smoothened-independent manner. *J Biol Chem* 279, 7064-71.

Therond, P., Alves, G., Limbourg-Bouchon, B., Tricoire, H., Guillemet, E., Brissard-Zahraoui, J., Lamour-Isnard, C., and Busson, D. (1996a). Functional domains of fused, a serine-threonine kinase required for signaling in Drosophila. *Genetics* 142, 1181-98.

Therond, P. P., Knight, J. D., Kornberg, T. B., and Bishop, J. M. (1996b). Phosphorylation of the fused protein kinase in response to signaling from hedgehog. *Proc Natl Acad Sci U S A* 93, 4224-8.

van den Heuvel, M., and Ingham, P. W. (1996). smoothened encodes a receptor-like serpentin protein required for hedgehog signalling. *Nature* 382, 547-551.

van Leeuwen, F., Samos, C. H., and Nusse, R. (1994). Biological activity of soluble wingless protein in cultured Drosophila imaginal disc cells. *Nature* 368, 342-4.

Vojtek, A. B., and Hollenberg, S. M. (1995). Ras-Raf interaction: two-hybrid analysis. *Methods Enzymol* 255, 331-42.

Wang, G., Amanai, K., Wang, B., and Jiang, J. (2000). Interactions with Costal2 and suppressor of fused regulate nuclear translocation and activity of cubitus interruptus. *Genes Dev* 14, 2893-905.

Wang, G., and Jiang, J. (2004). Multiple Cos2/Ci interactions regulate Ci subcellular localization through microtubule dependent and independent mechanisms. *Dev Biol* 268, 493-505.

Wang, Q. T., and Holmgren, R. A. (2000). Nuclear import of cubitus interruptus is regulated by hedgehog via a mechanism distinct from Ci stabilization and Ci activation. *Development* 127, 3131-9.

Wodarz, A., Hinz, U., Engelbert, M., and Knust, E. (1995). Expression of crumbs confers apical character on plasma membrane domains of ectodermal epithelia of Drosophila. *Cell* 82, 67-76.

Worby, C. A., Simonson-Leff, N., and Dixon, J. E. (2001). RNA interference of gene expression (RNAi) in cultured Drosophila cells. *Sci STKE* 2001, PL1.

Zhang, C., Williams, E. H., Guo, Y., Lum, L., and Beachy, P. A. (2004). Extensive phosphorylation of Smoothened in Hedgehog pathway activation. *Proc Natl Acad Sci U S A* 101, 17900-7.

Zhu, A. J., Zheng, L., Suyama, K., and Scott, M. P. (2003). Altered localization of Drosophila Smoothened protein activates Hedgehog signal transduction. *Genes Dev* 17, 1240-52.

LEGENDS

All the figures can be downloaded at: http://www.igmors.u-psud.fr/rousset/Plessis/

Figure 1: SMO and FU associate directly.

FU is composed of a N-terminal catalytic kinase domain (FU-KIN) followed by a regulatory domain (FU-REG) (aa 306-805, pale grey). A two-hybrid screen with FU-REG as bait led to the identification of 15 different prey clones encoding parts of the SMO C-terminus (horizontal arrows). SMO is a membrane protein with 7 transmembrane domains, an extracellular N-terminus and a cytoplasmic C-terminal tail. The smallest region of SMO that is sufficient for its interaction with FU (FU Binding Region or FU-BR) spans amino acids 985 to 1036 and is distinct from the COS2 binding region (COS2-BR, aa 557-686) determined by a two-hybrid assay (Lum et al., 2003), and from a cluster of phosphorylation sites for the PKA and CK1 (PKA/CK1-PS, aa 667-747) that was shown to be involved in SMO activation (Apionishev et al., 2005; Jia et al., 2004; Zhang et al., 2004).

ext: extracellular; int: intracellular.

Figure 2: Subcellular localisation of FU and SMO *in vivo*.

Confocal images of wing imaginal discs (A-H) or salivary glands (I) of *MS1096; UAS-GFP-smo* (A-D) or *MS1096; UAS-GFP-fu* flies (E-I).

(A) As reported for endogenous SMO and also shown in Figure 3A', GFP-SMO is preferentially stabilized in the posterior compartment. However, it also accumulates in the most anterior part of the wing pouch. (B-C) are high magnifications across the anterior/posterior (A/P) boundary. (C) is a confocal section acquired 24 µm below the section in (B). SMO-GFP accumulates at the surface on the apical side (B), whereas it is in vesicular structures that are more scattered elsewhere (C). No difference between the anterior and posterior compartments can be seen at the apical side, whereas in the more basal region, bigger vesicles are present in the anterior compartment. (D) Xz view reconstruction of the wing pouch across the A/P boundary shows the preferential apical localization of SMO. (E) GFP-FU is more abundant in the wing pouch anterior compartment. (F-G) High magnifications of apical (F) and mediane (G) views of the anterior region of the wing pouch. (G) is a confocal section acquired 38 µm below the section in (F). FU is diffused in the cytoplasm, but also accumulates at the plasma membrane on the apical side (arrow in enlarged insert in the upper right corner of F), and in vesicular puncta in the more basal region (arrow in enlarged insert in the upper right-hand corner of G). (H) Xz view reconstruction of the wing pouch across the A/P frontier confirms the apico-basal distribution of FU. (I) In salivary

glands, GFP-FU is present in the cytoplasm, in vesicle-like structures (arrow in enlarged insert in the lower right-hand corner). It also accumulates at the plasma membrane and in and around the nucleus (as also described in wing disc by Methot and Basler (Methot and Basler, 2000)).

All wing discs in this study are oriented with the anterior (Ant) to the left and the dorsal to the bottom. The A/P boundary is marked by an arrow head except in panel F and G, which are views of the anterior compartment. In all sections, scale bars equal 10 μm.

Note that *MS1096* is expressed at a higher level in the dorsal domain of the wing pouch (A and E).

Figure 3: SMO and FU co-localisation.

(A-C) Wing imaginal discs of *MS1096; UAS-GFP-fu* flies were dissected, fixed, permeabilized with Triton (0.3%) before immunolabelling of SMO. GFP-FU (A, B, C) and endogenous SMO (A', B', C') were sequentially detected by confocal microscopy. B" and C" correspond to overlaps showing both proteins. (A-A') Entire wing pouch: FU accumulates in cells of the anterior compartment (A), while SMO (A') is more abundant in the posterior compartment. (B-B'') and (C-C'') correspond to higher magnifications from median section of the anterior (B-B") and posterior (C-C") regions. Co-localization of both proteins occurs in some vesicular structures (yellow arrows) present in both compartments. SMO/FU co-localization was also observed in S2 cells (see Figure 4).

(D-H) Cl8 cells transiently expressing mRFP-FU alone (D), SMO-GFP alone (E), $SMO^{\Delta FU}$-GFP alone (F), mRFP-FU and SMO-GFP (G-G") or mRFP-FU and $SMO^{\Delta FU}$-GFP (H-H"). Red arrows correspond to mRFP-FU punctate structures, green arrows to SMO-GFP or $SMO^{\Delta FU}$-GFP vesicles and yellow arrows to vesicles co-labelled by both proteins. Note that no co-labelling can be observed between mRFP-FU and $SMO^{\Delta FU}$-GFP.

Scale bars equals 50 μm in A and 5 μm in B to H.

Figure 4 : SMO and FU colocalize independently from COS2. S2 cells transiently expressing mRFP-FU and SMO-GFP in the presence of endogenous COS2 (A -A'') or after *cos2* silencing by RNA interference (B-B'). In both cases, mRFP-FU and Smo-GFP strongly co-localize. See Figure 3S for *cos2* silencing.

Figure 5: Overexpression of SMO$^{\Delta FU}$ in the imaginal disc disrupts normal wing patterning.

(A) Wild-type wing. (B-E) Wings resulting from the over-expression of *UAS-GFP-smo* (B, C) or *UAS-smo$^{\Delta FU}$* (D, E) driven by *71B-GAL4* (B, D) or *MS1096* (C, E). Wing in (E) comes from a dissected imago.

Folds (represented by a star) are frequently encountered in the posterior compartment, probably due to differences in the sizes of the ventral and dorsal sides of the wing blade that result from a differential expression of *MS1096* (see Figure 2).

Wings over-expressing SMO are enlarged with a widening of the LV3-LV4 intervein typical of an activation of the HH pathway at the A/P. These effects are not visible here for SMO$^{\Delta FU,}$ due to the strong morphogenetic defects of the entire wing, although they can be observed in the case of lower activation (see Figure 6).

Here and in Figure 7, wings are oriented with the anterior to the top and the proximal end to the left.

2 to 5: LV2 to LV5

Figure 6: Over-expression of SMO$^{\Delta Fu}$ induces ectopic activation of HH pathway.

(A-B) *dpp-lacZ* (immunodetection of nuclear β-galactosidase, red in A and B) and *ptc* (immunodetection of PTC protein, blue in A' and B') expression in wing imaginal discs expressing *GFP-smo* (A) or *smo$^{\Delta FU}$* (B) driven by *MS1096*. (A'') and (B'') are respectively merged of (A-A'), and of (B-B').

(C-D) Anterior and posterior clones of SMO$^{\Delta FU}$ expressing cells (GFP, C and D) ectopically accumulate PTC (C') and EN (D') in a cell-autonomous manner. Merge in C" and D", respectively. Note that SMO$^{\Delta FU}$ clones distant from the A/P boundary, (C-C'') cause overgrowth of anterior tissue. Posterior clones have no effect.

(E-F) CI-FL immunodetection (with 2A1 antibody) in wild-type (E) or SMO$^{\Delta FU}$ (F) over-expressing disc.

(G-G'') Expression of SMO$^{\Delta FU}$ in anterior *smo^{D16}/Smo^{D16}* clones induces ectopic PTC expression and CI stabilization. The clones were generated by the MARCM system are positively marked by the GFP (green in G'') and stained for CI-FL (red in G, G''), PTC (blue, in G', G'').

All pictures are confocal sections, except for E and F, which are epifluorescence images. To better visualize the anterior end labelling, the contrast was increased in D-D''.

Figure 7: Activation of the HH pathway by SMO and SMO$^{\Delta FU}$ over-expression in *fu* mutant wings.

(A) *fu^{RX2} /Y; 71B* wing. LV3 and LV4 are distally and proximally fused (arrows) with a narrowing of LV3-4 intervein. (B) +//*Y; UAS-smo$^{\Delta FU}$/71B* wing. LV3 is thickened and cross-veins appear between LV2 and LV3 (star). (C) *fu^{RX2}*/*Y*; *UAS-smo$^{\Delta FU}$/71B* wing. Both the *fu*-phenotype and the *SMO$^{\Delta FU}$* over-expression effect are suppressed (compare with the wild-type wing in Figure 4A). (D) *fu^{RX2}*/+, *UAS-smo$^{\Delta FU}$/71B* wing. The effect of the SMO$^{\Delta FU}$ over-expression phenotype is partially suppressed, only a small cross-vein between LV3 and LV4 persists. (E) + */Y; UAS-GFP-smo*/*71B* wing with a small ectopic cross-vein (star). (F) *fu^{RX2}*/*Y*; *UAS-GFP-smo*/*71B* wing with a wild-type phenotype. Note that with both SMO and SMO$^{\Delta FU}$, the wings are enlarged with a widening of the LV3-LV4 intervein typical of an activation of the HH pathway at the A/P and that these effects are suppressed by *fu* mutations.

The same results are also observed in *fu^{1}* and *fu^{M1}* mutants (see Supplementary data Figure 5S).

Figure 8: A model for SMO and FU in the HH pathway.

In the absence of HH signal, SMO's activating effects are prevented by its endocytosis and targeting to the lysosome. We propose that the last 59 amino acids of SMO participate in its inhibition to reinforce the inactivated state of the pathway in the absence of signal. FU's negative effects might rely on SMO association with FU, which could thus phosphorylate SMO to modulate its trafficking and/or to prevent its phosphorylation by the PKA and CKI. The detection of changes in SMO trafficking would require a better characterization of the vesicles containing the wild type or truncated forms of SMO.

In response to HH, the inhibitory effects of both PTC and FU would be alleviated, and SMO is activated. In this situation, FU acts as an effector of SMO and is required for full activation of CI.

ext: extracellular; int : intracellular.

SUPPLEMENTARY DATA

The supplementary data includes 5 figures and their legend.

Figure 1S: The GFP-FU protein can rescue the *fu* mutant wing phenotypes.

(A) Wild-type wing.

(B) *fu^1/Y ; UAS-GFP-fu/+ ; TM3Sb/+* wing.

(C, D) *fu^1/Y* ; *UAS-GFP-fu*/+ ; *da-gal4*/+ wings: most wings display a total rescue of *fu* phenotype (C), only a few wings still show a weak *fu* phenotype (D).

Note also that GFP-FU was preferentially accumulated in the anterior wing disc cells (see Figure 2A and 3A) as reported for the endogenous FU protein (Ruel *et al.*, 2003).

Figure 2S: Preferential apical subcellular localisation of FU and SMO.

(A**)** Xz view reconstruction of GFP-FU over-expressed wing disc. Armadillo (ARM, in red) protein labelled with anti-ARM (N27A1, from DSHB), marks the apical side of the columnar epithelium.

(B) Xz view reconstruction of a GFP-FU (green) expressing disc. Endogenous SMO is immunodetected (red). The peripodial membrane, which also expresses endogenous SMO, is indicated by arrow and confirms the disc orientation.

Figure 3S: COS2 co-localizes with SMO and $SMO^{\Delta FU}$ in response to HH.

Cl8 cells transiently expressing mRFP-COS2 (A-A''), mRFP-COS2 with SMO-GFP (B-B'' and C-C'') or mRFP-COS2 with $SMO^{\Delta FU}$-GFP (D-D'' and E-E''). In A', C-C'' and E-E'': cells were co-transfected with pDAhh which encodes full-length HH. In the absence of HH, mRFP-COS2 is diffuse in the cytoplasm with a stronger accumulation in punctate structures. This localization is unaffected by HH. In cells co-transfected with mRFP-COS2

along with SMO-GFP or $SMO^{\Delta FU}$-GFP, mRFP-COS2 is still in punctate structures and almost no co-localization can be seen between COS2 and either form of SMO. Careful examination indicates that mRFP-COS2 and SMO are sometimes present in adjacent structures. When HH is present, co-tranfection of SMO-GFP or $SMO^{\Delta FU}$-GFP leads to the accumulation of mRFP-COS2 at the plasma membrane. Thus, the capacity of SMO to interact with COS2 is not affected by the lost of the last 59 aa of SMO.

Figure 4S: Western blot analysis of COS2 present in extracts made from the same amount of S2 cells (–, left lane) or S2 cells submitted to RNAi interference with a *cos2* dsRNA (+, right lane). The extracts were immunoblotted with anti COS2 antibody given by Ruel and Therond (Ruel et al., 2003). The upper band, which is not affected by RNAi treatment, is probably not specific, while the two other bands, whose intensity is strongly reduced by RNAi treatment, can be attributed to COS2. Considering their respective molecular masses, the intermediate band is likely to correspond to full-length COS2 and the lower band to a degradation product of COS2 . The molecular masses are indicated on the left.

Figure 5S: Activation of the HH pathway by SMO and $SMO^{\Delta FU}$ over-expression in fu^{M1} (A, B) and fu^{1} (C, D) mutant wings.

Driver: 71B
For legends see Figure 7

	(A) % of vesicular FU	(B) % vesicles			(C) SMO+ FU+ Pearson correlation coefficient (randomised value)
		SMO+FU-	SMO-FU+	SMO+FU+	
mRFP-FU	44 ± 13 (n=17)	-	-	-	-
SMO-GFP	-	-	-	-	-
$SMO^{\Delta FU}$-GFP	-	-	-	-	-
mRFP-FU + SMO-GFP	40 ± 14 (n=20)	25	22	53	0.845 ± -0.042 (- 0.062 ± -0.028)
mRFP-FU + $SMO^{\Delta FU}$-GFP	10 ± 7 (n=23)	88	10	2	0.053 ± -0.051 (- 0.266 ± - 0.038)

Table I: FU and SMO distribution in transfected Cl8 cells.

The distribution of mRFP-FU and SMO-GFP (or $SMO^{\Delta FU}$-GFP) in transiently transfected Cl8 cells expressing both proteins, either separately or together, was quantified as follows:

(A) % of vesicular FU: the intensity of vesicular mRFP-FU was compared to the total cellular mRFP-FU fluorescence. The number in brackets indicates the number of imaged cells analyzed.

(B) % of SMO+FU-, SMO-FU+ and SMO+FU+ vesicles: the number of vesicles labelled with SMO-GFP (or $SMO^{\Delta FU}$-GFP) alone (SMO+FU-), mRFP-FU alone (SMO+FU-) or both proteins (SMO+FU+) was compared to the total number of vesicles.

(C) Comparison of the profile distribution of mRFP-FU and SMO-GFP (or $SMO^{\Delta FU}$-GFP) by the Pearson correlation coefficient**.** The calculation was done for 10 vesicles. The values obtained after randomization of the mRFP-FU distribution are indicated in brackets.

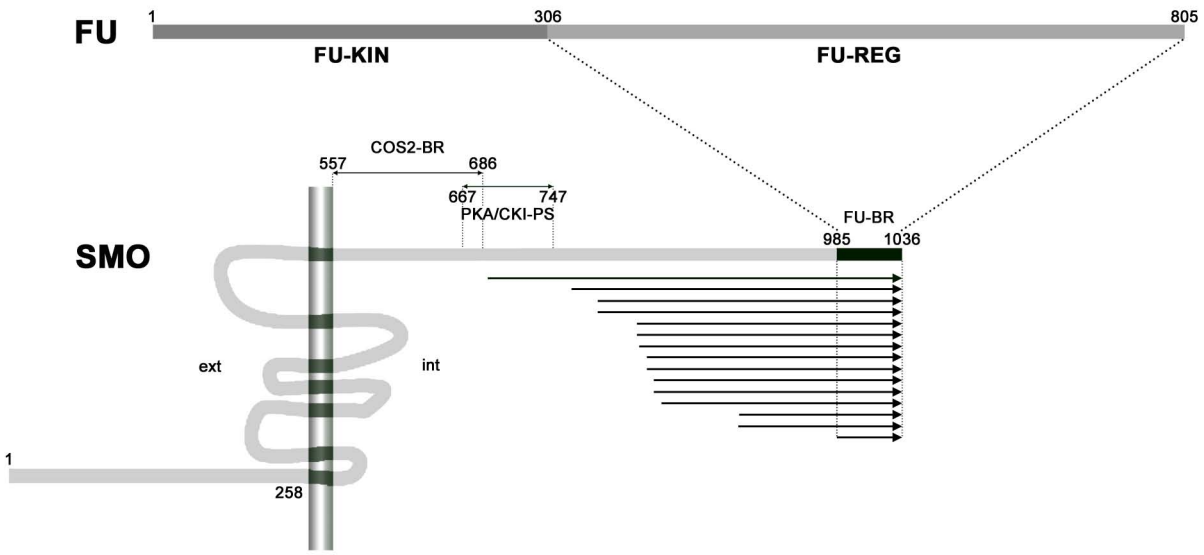
FU
1
306
805
FU-KIN
FU-REG
COS2-BR
557
686
667
747
PKA/CKI-PS
FU-BR
985
1036
SMO
ext
int
1
258

Figure 1

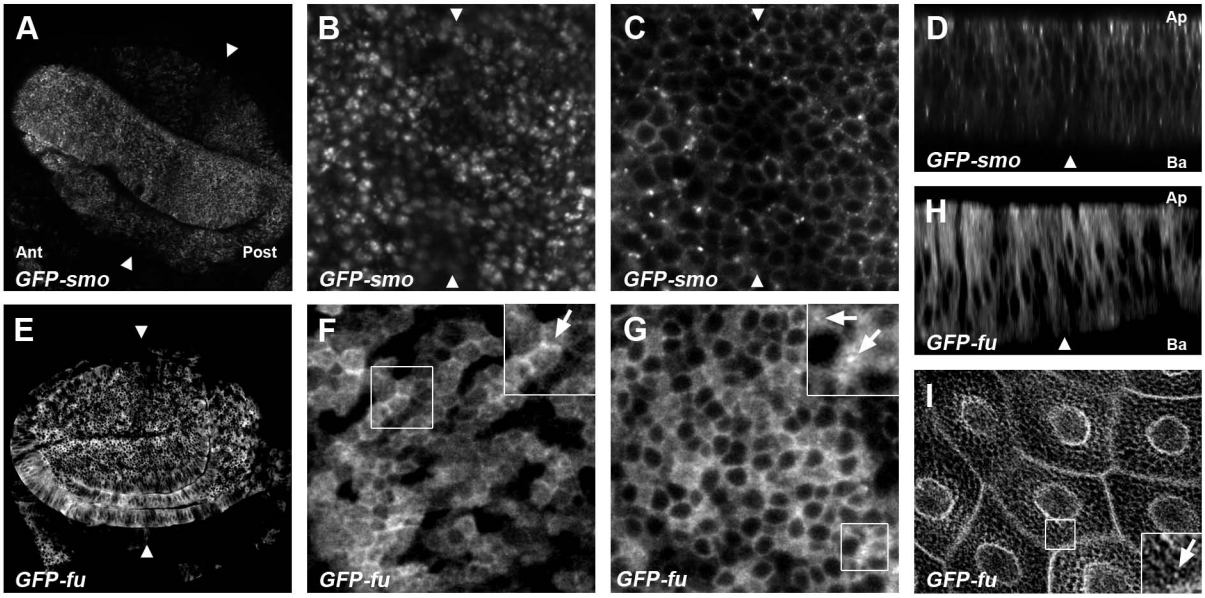
A
Ant
Post
GFP-smo
B
GFP-smo
C
GFP-smo
D
Ap
GFP-smo
Ba
H
Ap
GFP-fu
Ba
E
GFP-fu
F
GFP-fu
G
GFP-fu
I
GFP-fu

Figure 2

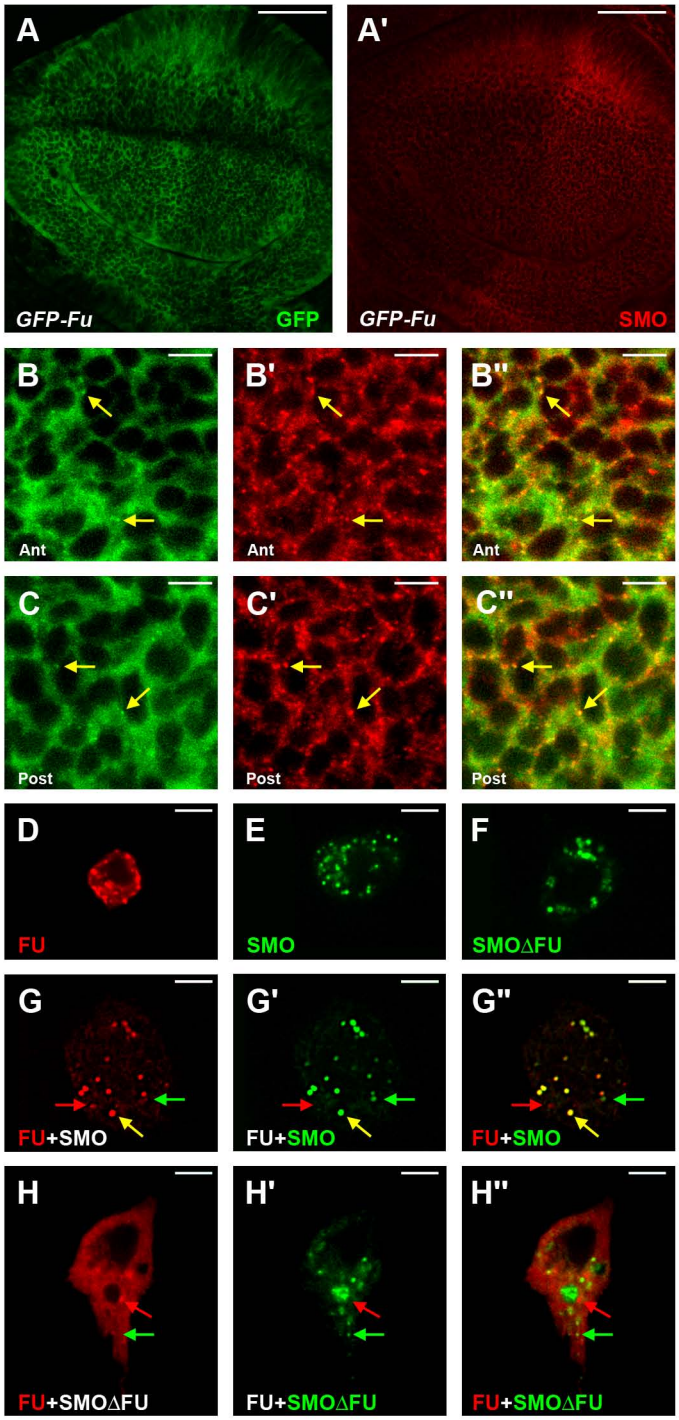
A
GFP-Fu
GFP
A'
GFP-Fu
SMO
B
Ant
B'
Ant
B''
Ant
C
Post
C'
Post
C''
Post
D
FU
E
SMO
F
SMOΔFU
G
FU+SMO
G'
FU+SMO
G''
FU+SMO
H
FU+SMOΔFU
H'
FU+SMOΔFU
H''
FU+SMOΔFU

Figure 3

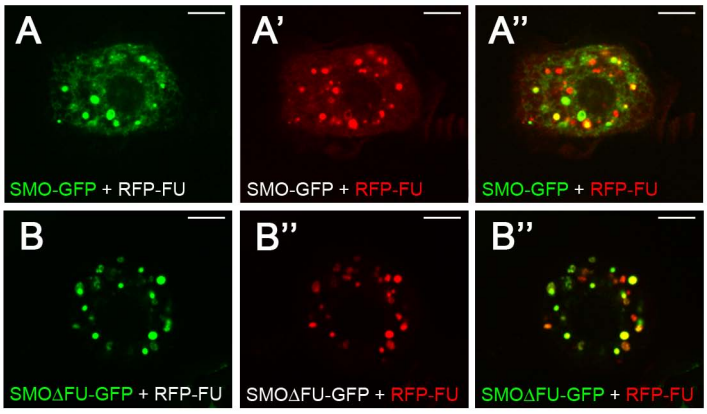
A
SMO-GFP + RFP-FU
A'
SMO-GFP + RFP-FU
A''
SMO-GFP + RFP-FU
B
SMOΔFU-GFP + RFP-FU
B''
SMOΔFU-GFP + RFP-FU
B''
SMOΔFU-GFP + RFP-FU

Figure 4

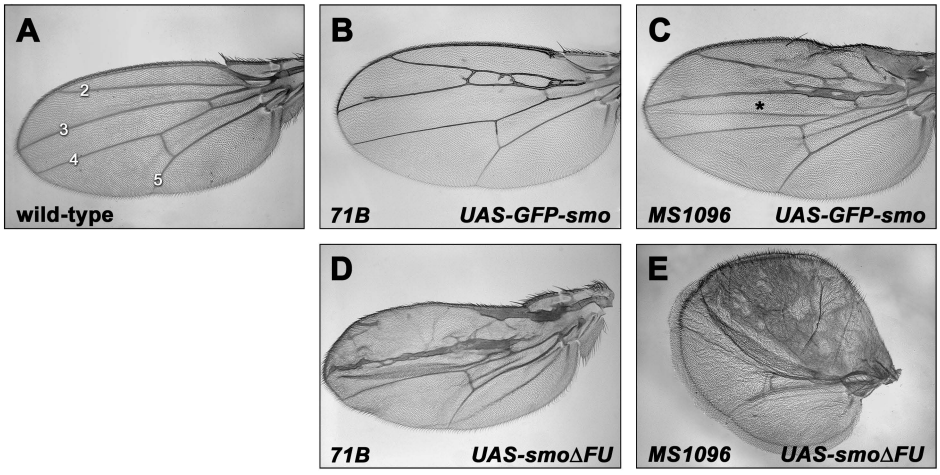
A
2
3
4
5
wild-type
B
71B
UAS-GFP-smo
C
*
MS1096
UAS-GFP-smo
D
71B
UAS-smoΔFU
E
MS1096
UAS-smoΔFU

Figure 5

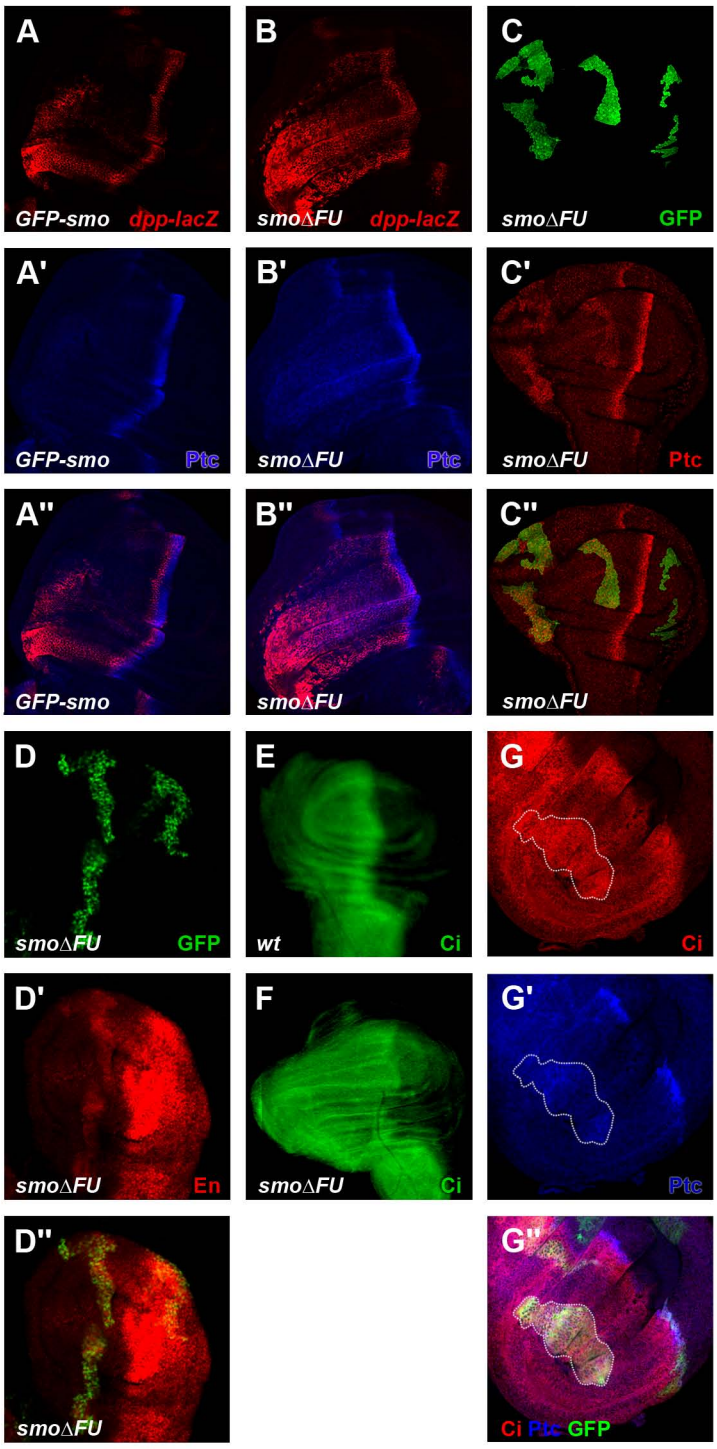
A
GFP-smo dpp-lacZ
B
smoΔFU dpp-lacZ
C
smoΔFU GFP
A'
GFP-smo Ptc
B'
smoΔFU Ptc
C'
smoΔFU Ptc
A''
GFP-smo
B''
smoΔFU
C''
smoΔFU
D
smoΔFU GFP
E
wt Ci
G
Ci
D'
smoΔFU En
F
smoΔFU Ci
G'
Ptc
D''
smoΔFU
G''
Ci Ptc GFP

Figure 6

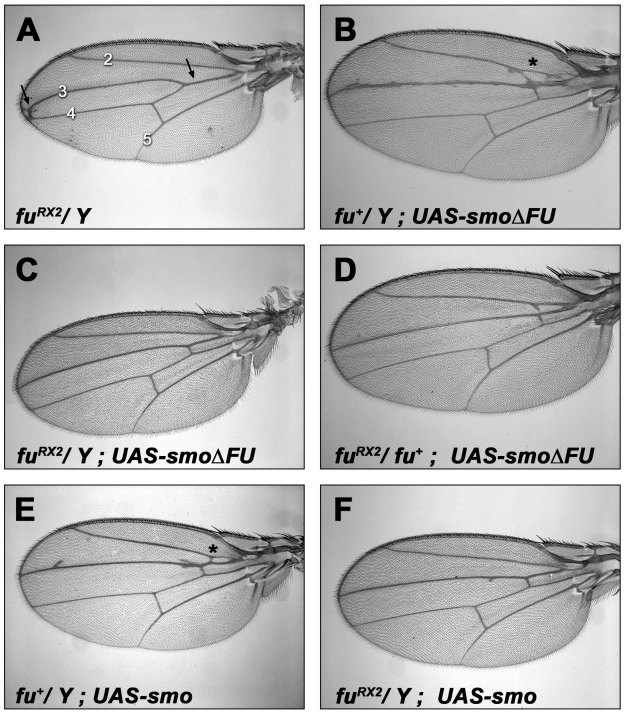
A
2
3
4
5
fu^RX2/ Y
B
*
fu+/ Y ; UAS-smoΔFU
C
fu^RX2/ Y ; UAS-smoΔFU
D
fu^RX2/ fu+ ; UAS-smoΔFU
E
*
fu+/ Y ; UAS-smo
F
fu^RX2/ Y ; UAS-smo

Figure 7

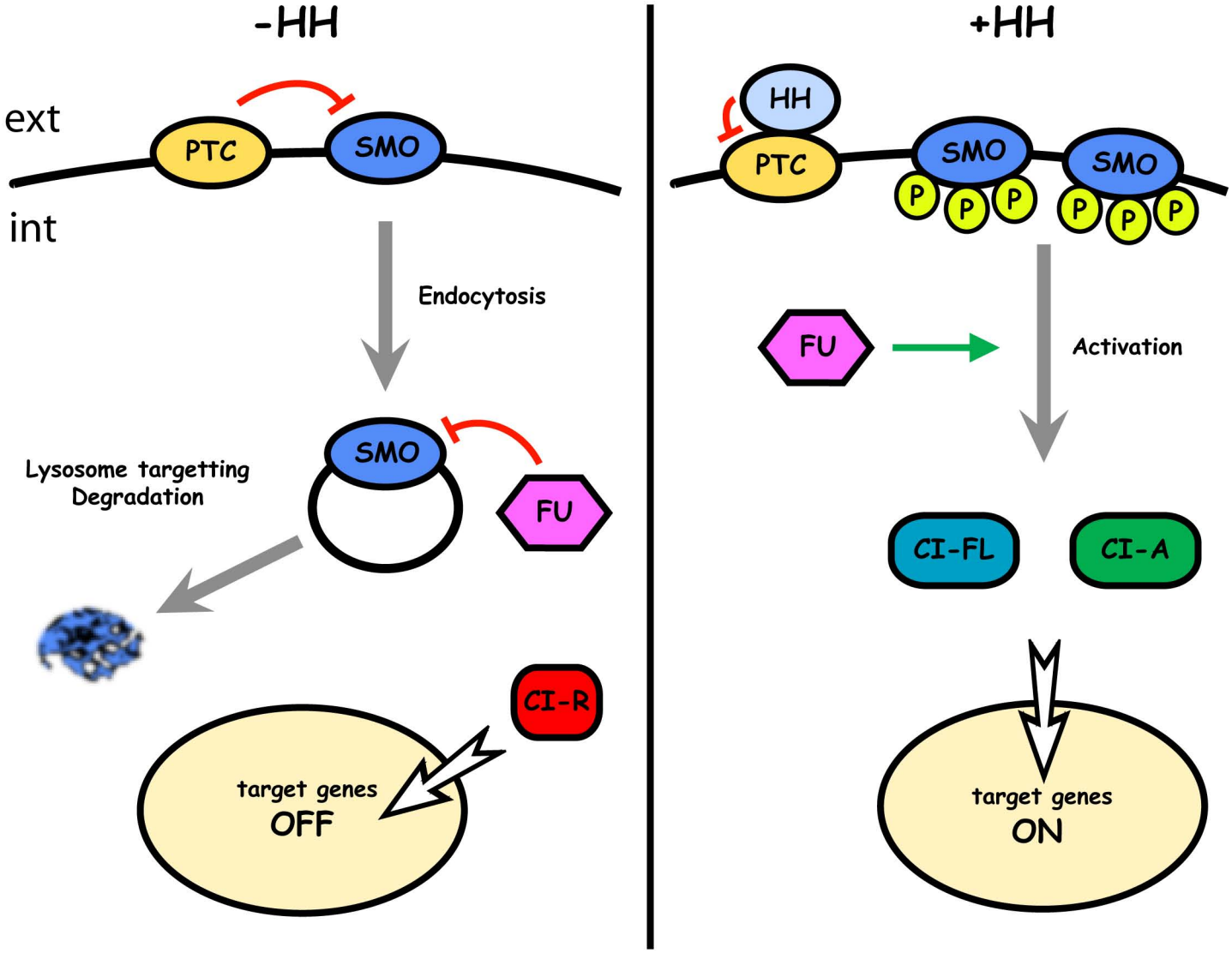
-HH
+HH
ext
int
PTC
SMO
HH
P
Endocytosis
Activation
FU
Lysosome targetting
Degradation
CI-FL
CI-A
CI-R
target genes
OFF
target genes
ON

Figure 8

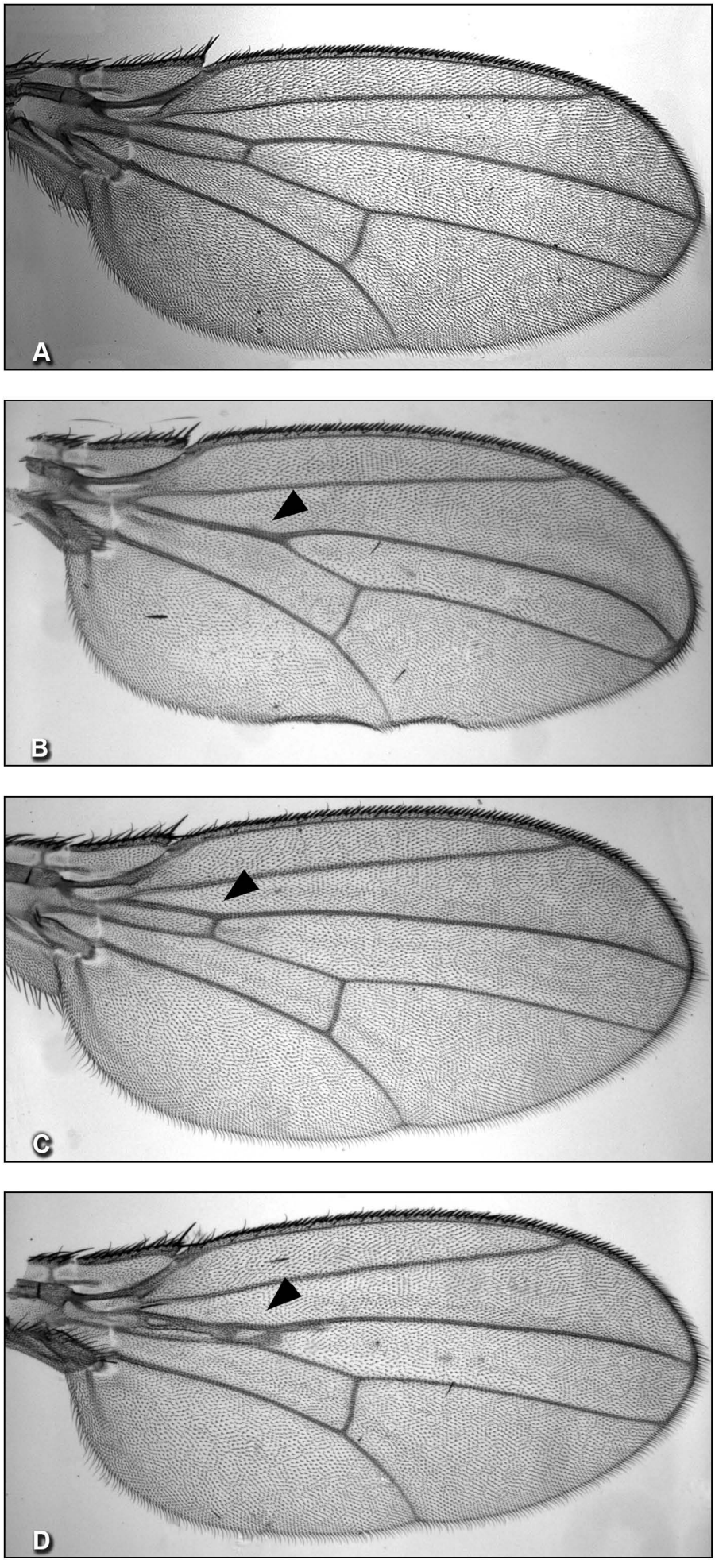

Figure 1s

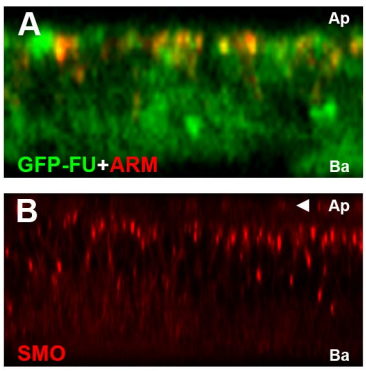

Figure 2s

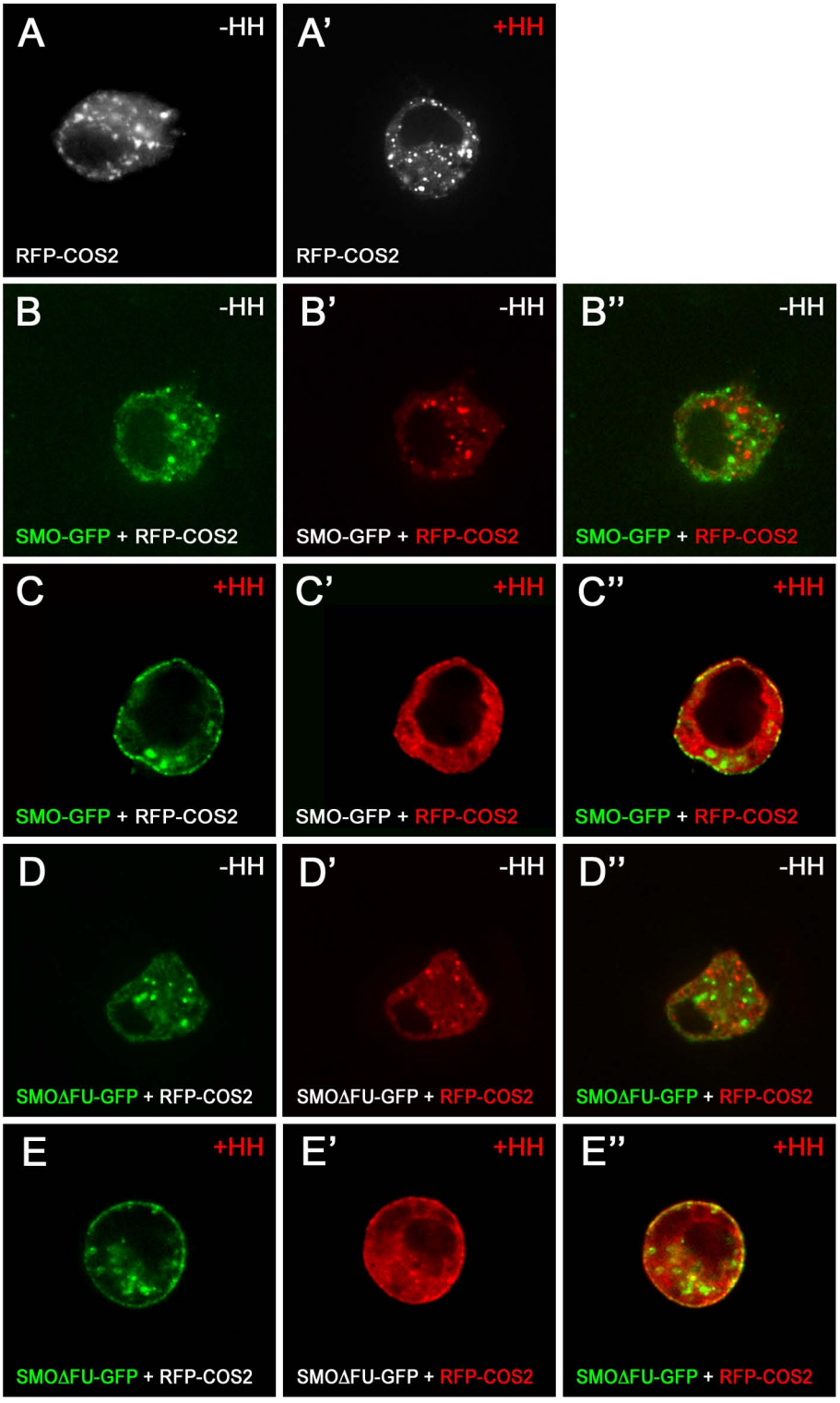
A
-HH
RFP-COS2
A'
+HH
RFP-COS2
B
-HH
SMO-GFP + RFP-COS2
B'
-HH
SMO-GFP + RFP-COS2
B''
-HH
SMO-GFP + RFP-COS2
C
+HH
SMO-GFP + RFP-COS2
C'
+HH
SMO-GFP + RFP-COS2
C''
+HH
SMO-GFP + RFP-COS2
D
-HH
SMOΔFU-GFP + RFP-COS2
D'
-HH
SMOΔFU-GFP + RFP-COS2
D''
-HH
SMOΔFU-GFP + RFP-COS2
E
+HH
SMOΔFU-GFP + RFP-COS2
E'
+HH
SMOΔFU-GFP + RFP-COS2
E''
+HH
SMOΔFU-GFP + RFP-COS2

Figure 3s

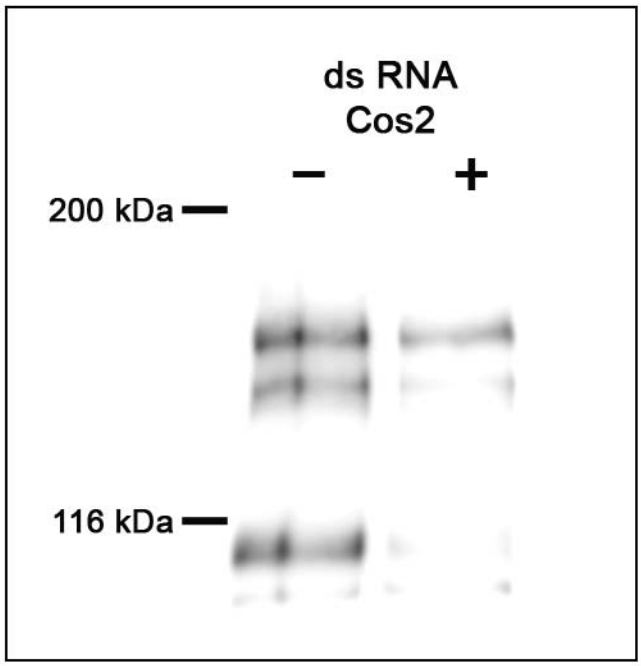

Figure 4s

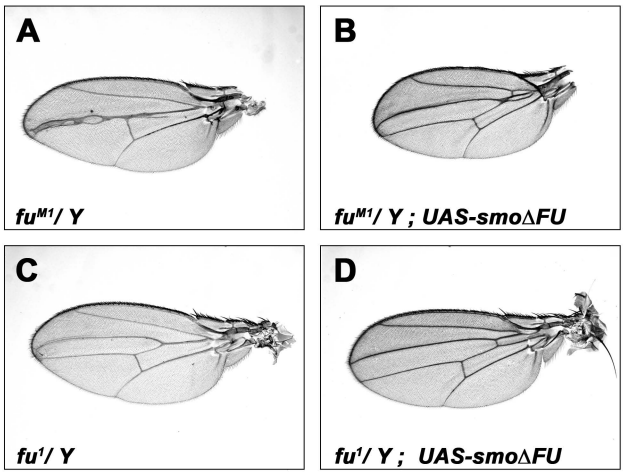

Figure 5s